Fractional Order Butterworth Filter: Active and Passive Realizations

A. Soltan Ali, A. G. Radwan, *Senior Member, IEEE*, and Ahmed M. Soliman, *Life Senior Member, IEEE*

***Abstract*—This paper presents a general procedure to obtain Butterworth filter specifications in the fractional-order domain where an infinite number of relationships could be obtained due to the extra independent fractional-order parameters which increase the filter degrees-of-freedom. The necessary and sufficient condition for achieving fractional-order Butterworth filter with a specific cutoff frequency is derived as a function of the orders in addition to the transfer function parameters. The effect of equal-orders on the filter bandwidth is discussed showing how the integer-order case is considered as a special case from the proposed procedure. Several passive and active filters are studied to validate the concept such as Kerwin–Huelsman–Newcomb and Sallen–Key filters through numerical and Advanced Design System (ADS) simulations. Moreover, these circuits are tested experimentally using discrete components to model the fractional order capacitor showing great matching with the numerical and circuit simulations.**

***Index Terms*—Butterworth filter, fractance, fractional-order circuit, fractional-order filter, Kerwin–Huelsman–Newcomb (KHN) filter, Sallen–Key filter, stability analysis.**

I. Introduction

FRACTIONAL calculus, the branch of mathematics which is concerned with differentiations and integrations of non-integer order, has been steadily migrating from the theoretical realms of mathematicians to many applied and interdisciplinary branches of engineering. As a result, huge attention has been paid to fractional calculus and its applications in various fields such as control design [1]–[6], electrical circuits [7]–[14], stability analysis [15]–[17], mechanics [18], electromagnetic [19]–[23], and bioengineering [24], [25]. This revolution has been greatly improved by the great effort of many scientists in many fields to realize the fractional-element or the so called constant phase element (CPE) [26]–[29]. The Riemann–Liouville definition of the fractional [1]–[4] derivative is given by

$$\frac{\mathrm{d}^\alpha}{\mathrm{d}t^\alpha}\mathrm{f(t)} \equiv \mathrm{D}^\alpha \mathrm{f(t)} = \frac{1}{\Gamma(1-\alpha)}\frac{\mathrm{d}}{\mathrm{dt}}\int_0^{\mathrm{t}} (\mathrm{t}-\tau)^{-\alpha}\mathrm{f}(\tau)\mathrm{d}\tau \quad (1)$$

Manuscript received February 07, 2013; revised April 17, 2013; accepted May 13, 2013. Date of publication June 18, 2013; date of current version September 09, 2013. This paper was recommended by Guest Editor B. Maundy.

A. Soltan Ali is with the Electrical Engineering Department, Faculty of Engineering, Fayoum University, Fayoum, Egypt (e-mail: asa03@fayoum.edu.eg).

A. G. Radwan, is with the Engineering Mathematics Department, Faculty of Engineering, Cairo University, and also with NISC Research Center, Nile University, Cairo, Egypt (e-mail: agradwan@ieee.org).

A. M. Soliman is with the Electronics and Communication Engineering Department, Faculty of Engineering, Cairo University, Cairo, Egypt (asoliman@ieee.org).

Digital Object Identifier 10.1109/JETCAS.2013.2266753

where $0 < \alpha \leq 1$. The Laplace transform of (1) at zero initial condition is as follows:

$$L\{D_t^\alpha f(t)\} = s^\alpha F(s). \quad (2)$$

Therefore, it is possible to define a fractance element as one whose impedance $Z(j\omega)$ is proportional to s^α as follows [26]–[29]:

$$Z(j\omega) \propto \omega^\alpha e^{\frac{j\alpha\pi}{2}}. \quad (3)$$

Conventionally, α has been restricted to $\{-1, 0, +1\}$ for the well-known circuit components: capacitor, resistor, and inductor, respectively. However, the fractional-element has many interesting properties where the phase angle is constant independent of the frequency, its magnitude versus frequency is nonlinear $(\alpha \neq 1)$ which can highlight or decrease the effect of frequency for $\alpha > 1$ and $\alpha < 1$, respectively. Moreover, the extra parameter α added to the circuit design can be used for further optimization, or design control.

Fractional order filters are represented by general fractional order differential equations, and considered as the generalized case of the integer-order filters. Fractional order filters were proposed in [7]–[11], where procedures for designing all filters with a fractional-element were introduced. Generally, there are two techniques to design the fractional order filter; the first one depends on the exact analysis using the fractional order elements [7]–[10], and the second procedure depends on the integer-approximation of these fractional elements which can be realized easily [11]. The analysis and implementation, using field programmable analogue array, for fractional order Butterworth filter of equal orders using the approximation transfer function was introduced in [11]. However, this procedure can be used only for fractional order filter with fractional order elements of the same fractional-order which decreases the degrees-of-freedom of the filter design.

This paper introduces the exact analysis of the fractional-order Butterworth filter of different orders, where the necessary condition is obtained as a function of the fractional-order parameters and the circuit elements. Therefore, the proposed technique considers the generalized case of the integer-Butterworth filter when all orders equal one. One of the main advantages of the proposed technique is that the extra degrees-of-freedom enrich the response so that an infinite number of relationships between the circuit parameters exist to achieve the Butterworth effect. In addition, the proposed fractional order should give the exact required frequency response of the filter and hence the expected response in the time domain. This exact response is vital for many applications especially those in which time is critical factor like the phase locked loop (PLL). Consequently, the fractional order Butterworth filter can be used with the PLL block to obtain the required response in the time domain and hence optimizing the PLL response.

The general analyses for the fractional-order filters having two different fractional elements with two different cases are introduced. Several numerical examples and stability analysis are presented and applied to different passive and active filters showing great matching. Finally, the experimental results of the discussed fractional-order filters are shown to validate the proposed procedure.

This work is organized as follows. Section II discusses the general procedure for the fractional order filter design. Then, the circuit design and simulation of the passive and active fractional order filter using ADS is shown in Section III. The experimental work is discussed in Section IV. Finally, Section V discusses the conclusion of this work.

II. Proposed Design Procedure

Butterworth filter approximation is one of the most widely used filter type because it has a number of interesting properties where the frequency response of the Butterworth low-pass filter is maximally flat in the pass-band [10], [30]–[33]. The magnitude squared function of the characteristic equation was introduced in [33] as

$$|D(j\omega)|^2 = 1 + \varepsilon\omega_n^{2N} \tag{4}$$

where N is a positive integer and represents the filter order and ω_n is the normalized frequency and ε is the attenuation in the pass-band and it is assumed to be unity in this paper. This work aims to deduce the generalized condition to achieve the fractional order Butterworth filter, where its frequency magnitude is given as

$$|D(j\omega)|^2 = 1 + \varepsilon\omega_n^{2m} \tag{5}$$

where m is any real positive value. Fractional order filters are characterized by their transfer function that contains a rational power of s in its characteristic polynomial.

The general form of the low pass fractional order filter transfer function is given by

$$T(s) = \frac{d}{s^{\alpha+\beta} + as^{\alpha} + bs^{\beta} + c} \tag{6}$$

where α and β are the fractional-orders and $0 < \alpha, \beta \leq 2$. When $s = j\omega$, the characteristic equation of (6) will be reduced to the following form:

$$\begin{aligned} \mathrm{D}(\mathrm{j}\omega,\beta,\alpha) = &\left(\omega^{\alpha+\beta}\cos\left(\frac{(\alpha+\beta)\pi}{2}\right)\right. \\ &\left. + \mathrm{a}\omega^{\alpha}\cos\left(\frac{\alpha\pi}{2}\right) + \mathrm{b}\omega^{\beta}\cos\frac{\beta\pi}{2} + \mathrm{c}\right) \\ &+ \mathrm{j}\left(\omega^{\alpha+\beta}\sin\left(\frac{(\alpha+\beta)\pi}{2}\right)\right. \\ &\left. + \mathrm{a}\omega^{\alpha}\sin\left(\frac{\alpha\pi}{2}\right) + \mathrm{b}\omega^{\beta}\sin\left(\frac{\beta\pi}{2}\right)\right). \end{aligned} \tag{7}$$

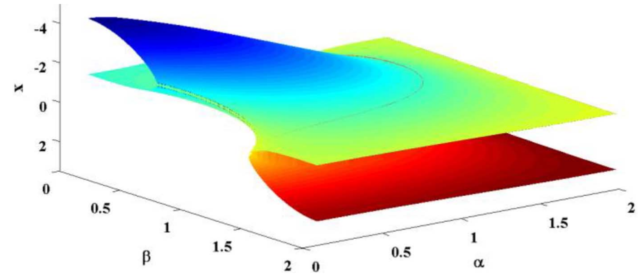

Fig. 1. Change in x with respect to α and β at $y = 0.9$.

To satisfy the Butterworth filter response, the magnitude squared of (7) must be reduced to the following form:

$$|\mathrm{D}(\mathrm{j}\omega,\beta,\alpha)|^2 \cong c^2 + \omega^{2(\alpha+\beta)}. \tag{8}$$

The cutoff frequency (ω_o) will be given by

$$\omega_{\mathrm{o}} = c^{\frac{1}{\alpha+\beta}}. \tag{9}$$

The condition to obtain Butterworth response at the cutoff frequency for a fractional order Butterworth filter is

$$\begin{aligned} &x^2 + y^2 + 2\left(\cos\frac{\beta\pi}{2} + \cos\frac{\alpha\pi}{2}\right)(x+y) \\ &\quad + 2xy\cos\left(\frac{(\alpha-\beta)}{2}\pi\right) + 2\cos\left(\frac{(\alpha+\beta)}{2}\pi\right) = 0 \end{aligned} \tag{10}$$

where $x = a\omega^{\alpha}/c$ and $y = b\omega^{\beta}/c$ are used to simplify the Butterworth condition. From (10), the condition of Butterworth filter depends on the fractional orders α and β in addition to the parameters x and y. So the design degree-of-freedom is increased and hence the design flexibility. Generally, for fixed parameters $\{a, b, \omega_0 \text{ and } c\}$, (10) will be a function of the fractional-orders α and β which gives an infinite number of solutions to achieve such filter.

Theoretically, the value of x can be positive or negative depending on the value of α and β for fixed values of y as shown in Fig. 1. Moreover, the stability analysis associated with the proposed fractional-order filter will be discussed using the technique proposed in [16]. Fig. 2(a) illustrates the poles movement for different values of $\alpha + \beta$ that satisfy the condition of the Butterworth response in (8) when $c = 1$ where the poles move on a circle of radius one. So, the filter poles can be obtained by using different combinations of the fractional orders, which increase the design degree-of-freedom.

In case of negative values of x; negative impedances; the filter will not have poles in the physical region of the s-plane when the fractional orders $\alpha + \beta < 1$, which means that the filter is stable for these combinations of the fractional orders. However, in case of positive x the system will be unstable when $\alpha + \beta < 1$. The positive solution of x for the condition (10) has a solution when $\alpha + \beta > 1$ and sometimes has two solutions for higher values of α and β, as shown in Fig. 2(b). It is worthy to note that the response of y with respect to α and β should be similar to the behavior of x because of the symmetry of (10).

Numerical simulation results of the FLPF are shown in Fig. 3(a) for different values of α and β after calculating the value of x using (10) for a fixed value of y.

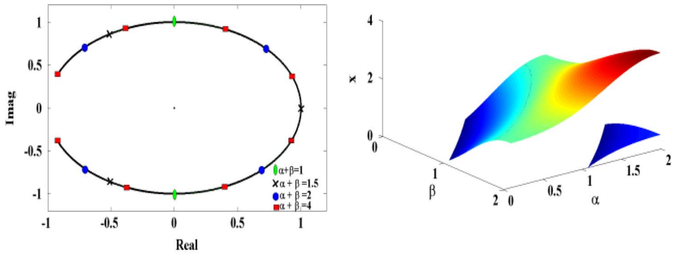

(a) (b)

Fig. 2. (a) Poles locations with respect to α and β when $c = 1$. (b) Change in x with respect to α and β at $y = 0.1$ for positive values of x.

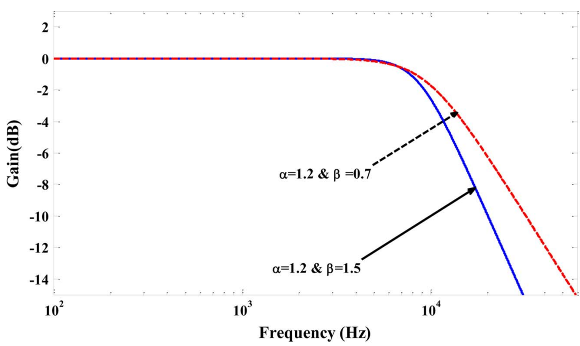

(a)

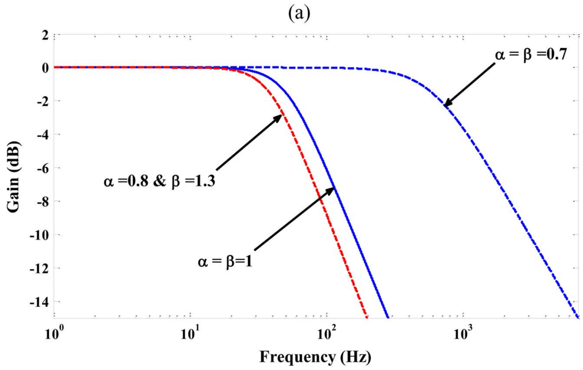

(b)

Fig. 3. (a) Magnitude response of the FLPF at different values of α and β at $y = 0.1$ at $\omega_o = 2\pi * 10$ krad/s. (b) Effect of the fractional orders on the bandwidth of Butterworth filter at $c = 10^5$.

From Fig. 3(a), the resulting filter response is maximally flat in the pass-band which satisfies the Butterworth response. It is clear that the slope of the Butterworth FLPF is proportional to the fractional orders as $(\alpha+\beta)$ dB per decade as shown in Fig. 3 which confirms that the cutoff frequency depends not only on the parameter c, but also on $\alpha+\beta$ as shown from (9). Therefore, the filter bandwidth can be controlled by the fractional orders without affecting the value of c as shown in Fig. 3(b). In the following subsections, two special cases of the transfer function of (6) are introduced for the case $\alpha = \beta$, and $b = 0$.

A. Case 1: Equal Order Fractional Butterworth Filter

In this case $\beta = \alpha$, and (8) can be written as

$$|D(j\omega,\alpha)|^2 \cong c^2 + \omega^{2N\alpha} \tag{11}$$

where N is the number of the fractional order elements. For the case of interest $N = 2$, the two variables a, b will be merged into one parameter χ where $\chi = a + b$. Therefore, the degrees-of-freedom decrease by two from the previous general case. The magnitude squared of the characteristic equation $|D(j\omega,\alpha)|^2$ can be rewritten as

$$\begin{aligned}|\mathrm{D}(j\omega,\alpha)|^2 &= \omega^{4\alpha} + 2\chi\omega^{3\alpha}\cos\left(\frac{\alpha\pi}{2}\right)\\ &+(\chi^2 + 2\mathrm{c}\cos\alpha\pi)\omega^{2\alpha} + 2\chi\mathrm{c}\omega^{\alpha}\cos\left(\frac{\alpha\pi}{2}\right) + \mathrm{c}^2.\end{aligned} \tag{12}$$

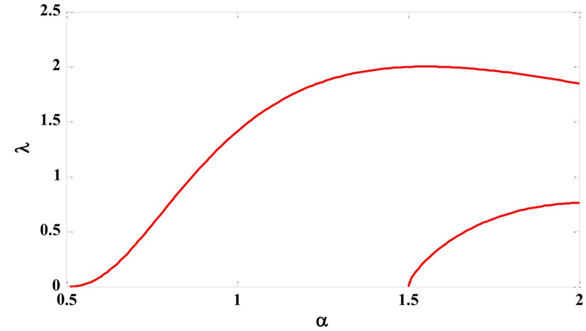

Fig. 4. Change in λ with respect to α for equal order Butterworth filter for case I.

Hence, after some simplifications the condition for the Butterworth filter will be as follows:

$$\rho\lambda^{2\alpha} + \left(\frac{1 + 2\rho\cos(\alpha\pi)}{2\cos(0.5\alpha\pi)}\right)\lambda^{\alpha} + 1 = 0 \tag{13}$$

where $\lambda^{\alpha} = (\chi/c)\omega^{\alpha}$ and $\rho = (c)/(\chi^2)$. From the above equations the cutoff frequency (ω_o) depends on c and α as follows:

$$\omega_o = c^{\frac{1}{2\alpha}}. \tag{14}$$

Therefore, the relationship between λ and ρ at the cutoff frequency is given by (15). Since (13) is a quadratic equation in λ^{α} and due to the constraint that λ should be positive, then the solution of (13) is given by (16) where three different cases are observed; no roots, single root, and double roots in the case of $0 < \alpha < 0.5, 0.5 \le \alpha < 1.5$, and $1.5 \le \alpha < 2.0$, respectively, are presented in Fig. 4

$$\rho = \frac{1}{\lambda^{2\alpha}} \tag{15}$$

$$\lambda = \begin{cases} 0 & 0 < \alpha < 0.5 \\ (-2\cos(0.5\alpha\pi) + \sqrt{2})^{\frac{1}{\alpha}} & 0.5 \le \alpha < 1.5 \\ (-2\cos(0.5\alpha\pi) \pm \sqrt{2})^{\frac{1}{\alpha}} & 1.5 \le \alpha < 2.0 \end{cases}. \tag{16}$$

Therefore, if the fractional power α is known, λ could be calculated. Although, (16) gives two values of λ at certain cases of α, but they produce the same poles of (11). This means that the poles do not depend on the value of λ as expected.

The performance of (12) is approximately equal to the performance of the canonical equation of Butterworth given in (11), as depicted in Fig. 5(a). Therefore, the condition of (13) is satisfied for the whole bandwidth of interest. Also, the numerical simulation of the proposed fractional order filter is presented in Fig. 5(b) for different values of α. In addition, the numerical simulation for the fractional order filters using the procedure proposed in [11] is shown in Fig. 5(b). The technique presented in [11] depends on using more poles and zeros to achieve the required response. Consequently, the procedure of [11] increases the transfer function complexity as shown in the transfer functions of (17) (a) and (b) for $\alpha = (1.7, 0.7)$, respectively.

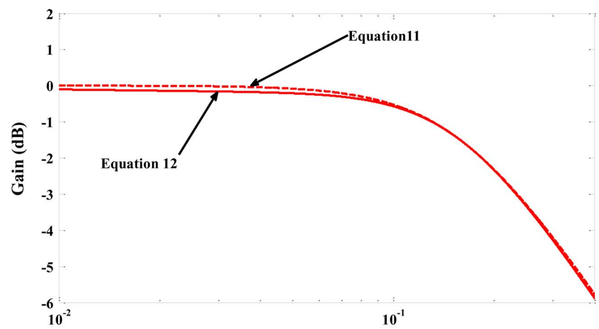

(a)

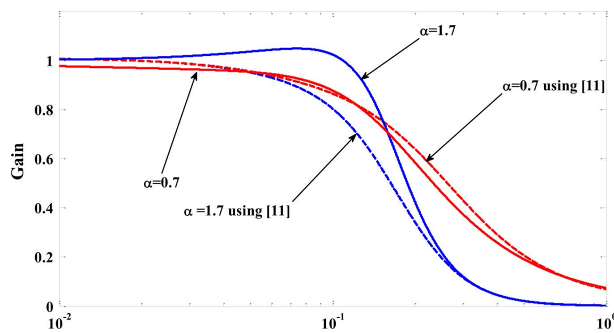

(b)

Fig. 5. (a) Magnitude response of (11) and (12) for $\alpha = 0.7$. (b) Magnitude response of the proposed filter and the filter of [11] at $\omega_o = 1$ rad/s.

Hence, this complexity in the transfer function leads to a complex circuit implementation. As shown in Fig. 5(b), the proposed method and the method of [11] produce very similar results for different values of α

$$T(s) = \frac{0.96s^2 + 7.68s + 3.36}{3.4s^5 + 15s^4 + 30s^3 + 30.3s^2 + 16s + 3.3} \quad (17a)$$

$$T(s) = \frac{0.96s^2 + 7.68s + 3.36}{3.4s^3 + 10.4s^2 + 11.7s + 3.33}. \quad (17b)$$

For the conventional case $\alpha = \beta = 1$, then the value of $\lambda = \sqrt{2}$, and $\rho = 0.5$ which is expected.

B. Case 2: $b = 0$

The transfer function of fractional order Butterworth filter in this case will be given as follows:

$$T(s) = \frac{d}{s^{\alpha+\beta} + as^{\alpha} + c} \quad (18)$$

where α and β are the fractional-orders and $0 < \alpha, \beta \leq 2$. To satisfy the Butterworth filter response, the magnitude response must be reduced to the following form:

$$|D(j\omega, \alpha, \beta)|^2 \cong \omega^{2(\alpha+\beta)} + c^2. \quad (19)$$

So, the cutoff frequency will be the same as that given in (9). To achieve the characteristic equation of (19), the following condition must be satisfied:

$$\lambda^{\alpha} + 2\rho\lambda^{\alpha+\beta}\cos\left(\frac{\beta\pi}{2}\right) + \rho\lambda^{\beta}\cos\left(\frac{(\beta+\alpha)\pi}{2}\right) + 2\cos\left(\frac{\alpha\pi}{2}\right) = 0 \quad (20)$$

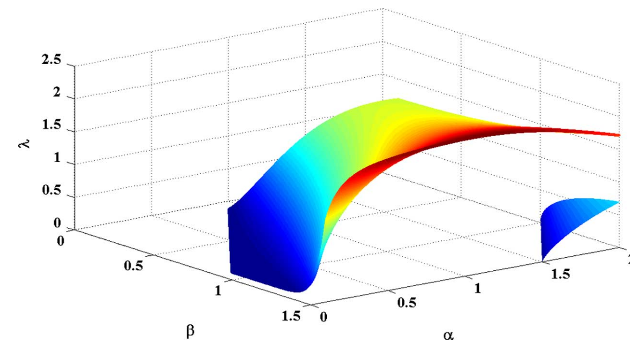

Fig. 6. Values of λ at different values of α and β for case II.

where $\lambda^{\alpha} = a\omega^{\alpha}/c$ and $\rho\lambda^{\beta} = \omega^{\beta}/a$ are used to simplify the Butterworth condition. By using the cutoff frequency, $\rho\lambda^{\alpha+\beta} = 1$ and the value of λ can be evaluated by

$$\lambda^{\alpha} = -\left(\cos\left(\frac{\beta\pi}{2}\right) + \cos\left(\frac{\alpha\pi}{2}\right)\right) \pm\sqrt{2 - \left(\sin\left(\frac{\alpha\pi}{2}\right) - \sin\left(\frac{\beta\pi}{2}\right)\right)^2}. \quad (21)$$

Therefore, the cutoff frequency and the Butterworth condition generally depend on the fractional orders besides the parameters a and c. So, the design degree-of-freedom and flexibility are increased. By applying simple trigonometric rules, then (21) has three cases as follows:

- no solution when $\alpha + \beta < 1$;
- single solution when $1 \leq \alpha + \beta < 3$;
- two solutions when $3 \leq \alpha + \beta < 4$.

Fig. 6 illustrates the values of λ as a surface versus $\alpha\beta$ plane where the three different cases appear. As expected, no solution exists for the case of $\alpha + \beta < 1$ and λ has two solutions when $3 \leq \alpha + \beta$.

This means two different filters for the same ω_o with Butterworth response will be obtained which increases the design flexibility. Moreover, the value of the phase at the cutoff frequency is given by (22) where the phase value depends on the fractional orders α and β only.

As a special case, when $\alpha = \beta$ the phase at the cutoff frequency is given by $\alpha\pi/2$. So, a specific value of the phase can be obtained at the cutoff frequency without affecting the values of the parameters a and b by changing only the fractional orders α and β

$$\tan\theta = \frac{-\tan\left(\frac{(\alpha-\beta)\pi}{4}\right) \pm \tan\left(\frac{\alpha\pi}{2}\right)\sqrt{0.5\tan^2\left(\frac{(\alpha-\beta)\pi}{4}\right) - 1}}{\tan\left(\frac{\alpha\pi}{2}\right)\tan\left(\frac{(\alpha-\beta)\pi}{4}\right) \pm \sqrt{0.5\tan^2\left(\frac{(\alpha-\beta)\pi}{4}\right) - 1}}. \quad (22)$$

Now, it is time to check the response of the fractional order Butterworth filter numerically. The frequency response of (19) is shown in Fig. 7 for different values of α and β after calculating the value of λ using (21). It is clear from Fig. 7 that the filter output satisfies the maximally flat response. Hence, the Butterworth condition of (21) is valid for a wideband of frequencies. In addition, the procedure of [11] cannot be used with

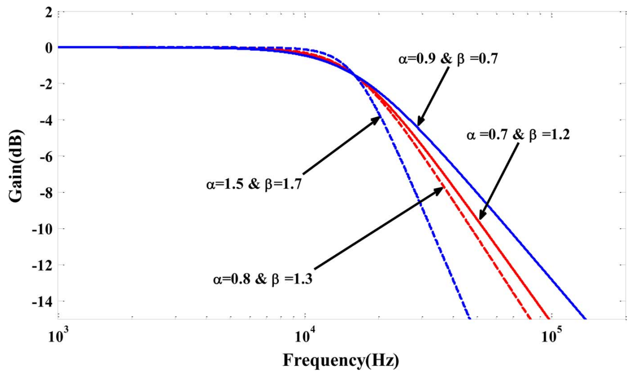

Fig. 7. Magnitude response for the ideal and the actual Butterworth response at different values of α and β for $\omega_o = 2\pi * 10^4$ rad/s.

this case $(b = 0)$ because the procedure of [11] is used only to design fractional order filters with fractional order elements of the same order. So, it is not possible to make a comparison between the proposed design procedure and the technique of [11] in this case.

III. Circuit Design and Simulation

The purpose of this section is to apply the proposed design procedure on practical filters. To model the fractional order element, a finite element approximation relies on the possibility of emulating a fractional-order capacitor of order 0.5 via semi-infinite RC trees [29]. The technique was later developed by the authors of [26]–[28] for any fractional order element of order less than unity $(\alpha < 1)$ as presented in Fig. 8(a). On the other hand, to obtain a fractional order element of order $\alpha > 1$, the GIC [31] of Fig. 8(b) can be used to obtain grounded fractional order elements. Yet, to produce floating fractional order capacitors or inductor, two cascaded GIC should be used. The input impedance for the grounded GIC is $Z_i = Z_L Z_1 Z_3 / Z_2 Z_4$. So, this model of the fractional order element is used to build and simulate the fractional order filters of different types. Consequently, in the following subsections the circuit simulation using ADS for fractional order passive filter realization and Kerwin–Huelsman–Newcomb (KHN) and Sallen–Key for the active realization are introduced. The relation between the circuit element values $\{R, L, C, \text{ and } \omega_o\}$ and the transfer function parameters $\{a, b, \text{ and } c\}$ are summarized in Table I.

A. Passive Realization

The passive implementation of the Butterworth filter is presented in the subplot of Fig. 8(c) using two fractional order elements of different orders.

The passive circuit transfer function is similar to that of the special cases mentioned before. So the algorithms of the special cases can be used to calculate the value of the transfer function parameters $\{a, c\}$. Hence, the relations given in Table I can be used to calculate the values of the circuit components. Besides, for the case of equal orders, Table II gives the value of L and C at $\mathrm{R} = 50\ \Omega$ and at the normalized frequency $\omega_h = 1$ rad/s. By using the frequency scaling [9], the value of L and C

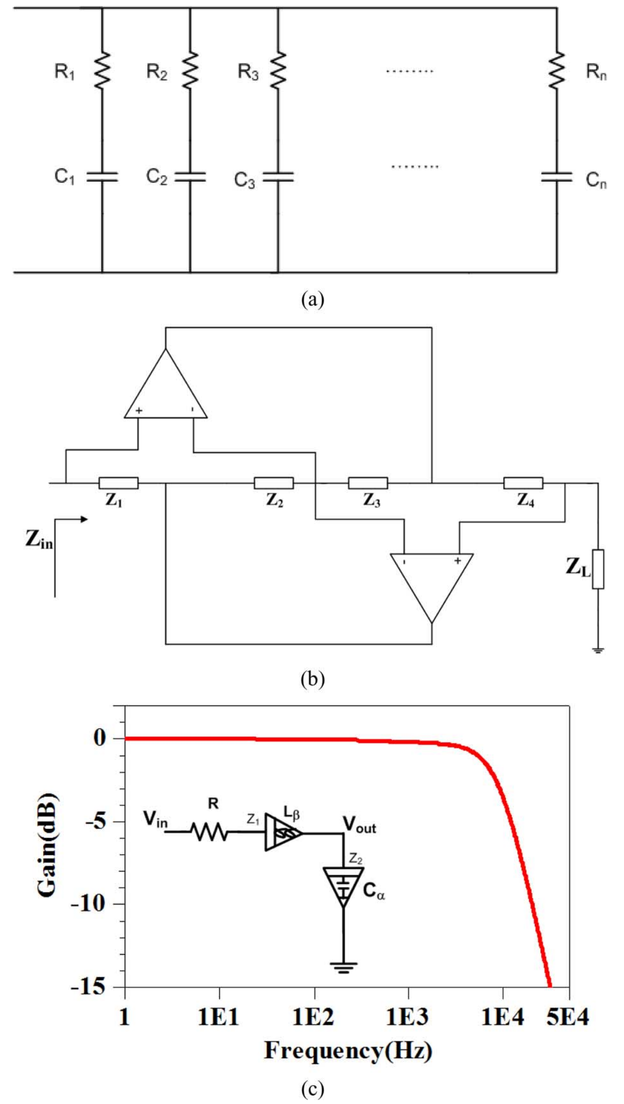

Fig. 8. (a) Approximation of a fractional capacitor via a self-similar tree used in ADS, (b) GIC circuit diagram, and (c) the circuit simulation results for the passive Butterworth filter for $\alpha = \beta = 0.7$ at $\omega_o = 2\pi * 10$ k rad/s.

TABLE I
Relation Between the Circuit Components and the Transfer Function Parameters

	a	b	c	ω_o
RLC circuit	R/L_β	0	$1/(L_\beta C_\alpha)$	$(L_\beta C_\alpha)^{\frac{-1}{\alpha+\beta}}$
KHN – filter	$\frac{R_3}{C_\beta R_1} \frac{(1+R_5/R_6)}{R_3+R_4}$	0	$\frac{R_5/R_6}{C_\alpha C_\beta R_1 R_2}$	$\left(\frac{R_5/R_6}{C_\alpha C_\beta R_1 R_2}\right)^{\frac{1}{\alpha+\beta}}$
Sallen – Key filter	$\frac{1-R_4/R_3}{R_2 C_\beta}$	$\frac{1}{R_2 C_\alpha} + \frac{1}{R_1 C_\alpha}$	$\frac{1}{C_\alpha C_\beta R_1 R_2}$	$\left(\frac{1}{C_\alpha C_\beta R_1 R_2}\right)^{\frac{1}{\alpha+\beta}}$

can be obtained at any cutoff frequency. For the fractional orders that have two values of λ, there are two combinations of the values for L and C that satisfy the Butterworth response. The circuit simulation for $(\alpha, \beta) = (0.7, 0.7)$ is illustrated in Fig. 8(c) which is very close to the numerical analysis presented before. Consequently, this indicates that the proposed design

TABEL II
VALUES OF L AND C FOR DIFFERENT α AT $R = 50\ \Omega$ AND $\omega_o = 1$ RAD/S

α	$L_\alpha(H/(sec)^{\alpha-1})$		$C_\alpha(F/(sec)^{\alpha-1})$	
0.7	98.77		0.01012	
0.8	62.8		0.0159	
0.9	45.4		0.0220	
1	35.36		0.02828	
1.1	28.95		0.03454	
1.2	24.6		0.0406	
1.3	21.53		0.0464	
1.4	19.31		0.0518	
1.5	17.68		0.0567	
1.6	16.49	245.28	0.0606	0.004077
1.7	15.64	135.96	0.0639	0.00736
1.8	15.077	102.48	0.0663	0.009758
1.9	14.75	89.1	0.06779	0.01122
2	14.64	85.35	0.06829	0.011717

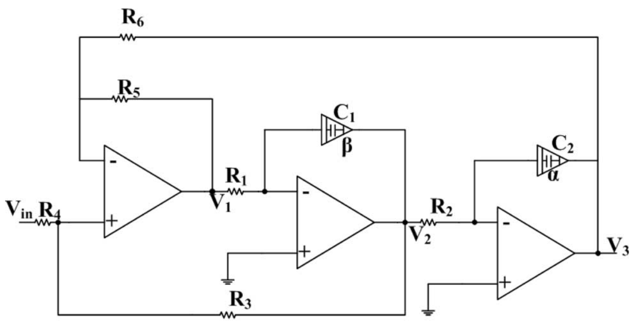

(a)

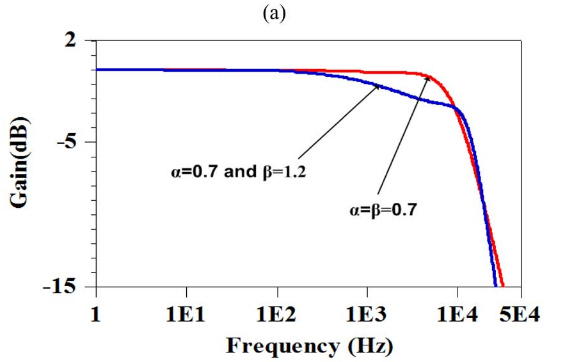

(b)

Fig. 9. (a) KHN filter using two elements of different orders. (b) Circuit simulation of the KHN filter at $\omega_o = 2\pi * 10$ krad/s.

procedures for the special cases gives very accurate and close results to the theoretical analysis.

B. Active Realization: KHN Filter

The fractional-order KHN filter where two normal capacitors are replaced by two fractional capacitors of different orders α and β is shown in Fig. 9(a). This section will focus on the simulation of KHN filter as its transfer function is similar to (18). Consequently, the two special cases presented before of equal orders and for $b = 0$ can be used here to design the filter. Then, the relation between the circuit elements and the parameters of the transfer function of (18) is given in Table I. The circuit simulation of the fractional order KHN filter is shown in Fig. 9(b). Two cases are presented in Fig. 9(b); the first one is based on the equal orders special case $(\alpha = \beta = 0.7)$. Therefore, the value of λ is determined by using (16). Hence, the value of a

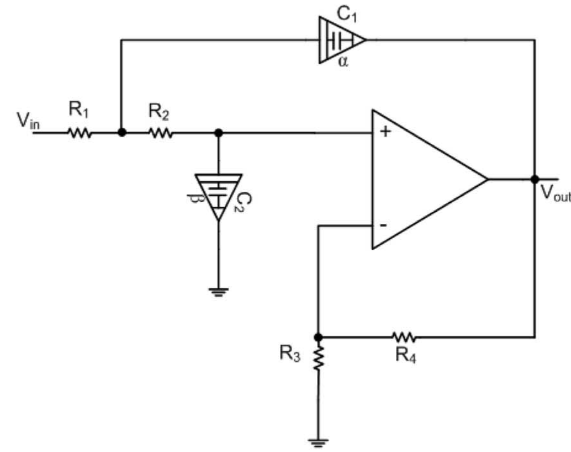

(a)

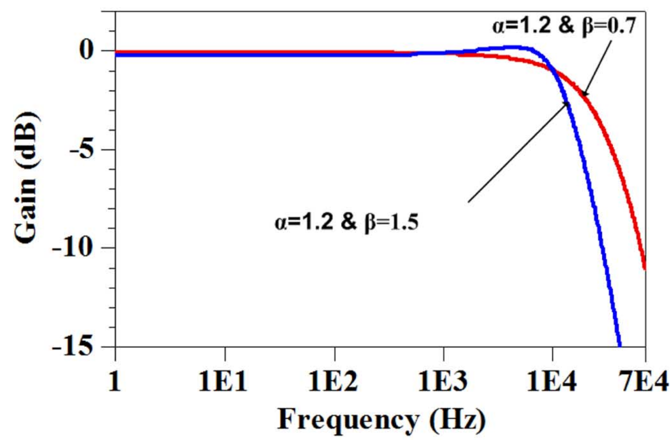

(b)

Fig. 10. (a) Circuit diagram of the fractional Sallen-Key filter. (b) Circuit simulation of the Sallen-Key filter of the subplot at $\omega_o = 2\pi * 10$ krad/s.

and c are calculated at the specified frequency to be as follows $(1.156 * 10^3, 5.22 * 10^6)$ for a and c, respectively, and from Table I, the components value can be calculated. Secondly, the special case 2 $(b = 0)$ is also used to design a fractional order KHN filter with the orders $(\beta, \alpha) = (1.2, 0.7)$.

So, (21) is used here to determine the value of λ and hence the value of the parameters a and c at the required cutoff frequency as follows $(a, c) = (7.246 * 10^5, 1.31 * 10^9)$. Then the value of the circuit elements is calculated using the relations given in Table I. by comparing Fig. 9(b), Fig. 7(b), the simulation results are very close to the numerical analysis. Finally, the procedure proposed in [11] cannot design the fractional order KHN circuit shown in Fig. 9(a) because the KHN transfer function is different from that of (17) for the same orders. Instead, the procedure of [11] will design its own filter circuit network.

C. Active Realization: Sallen–Key Filter

Sallen–Key filters are popular second-order filters, which employ a single op-amp as VCVS with dc gain G. A fractional-order Sallen–Key low-pass filter with two fractional order elements is shown in Fig. 10(a). Since, the transfer function of the Sallen–Key filter is similar to the general case of the proposed design procedure; the condition of (10) is used here to determine the parameters of the transfer function which satisfy the

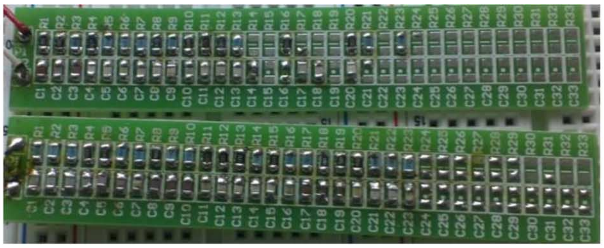

(a)

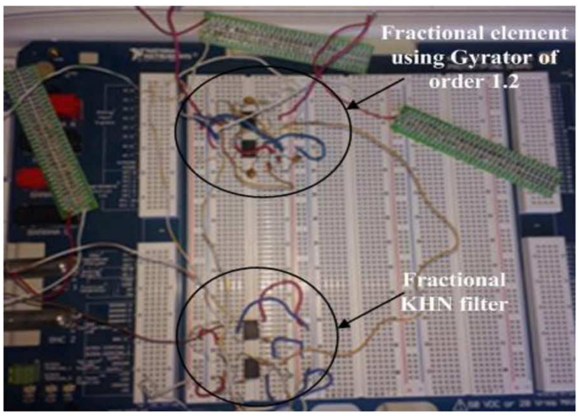

(b)

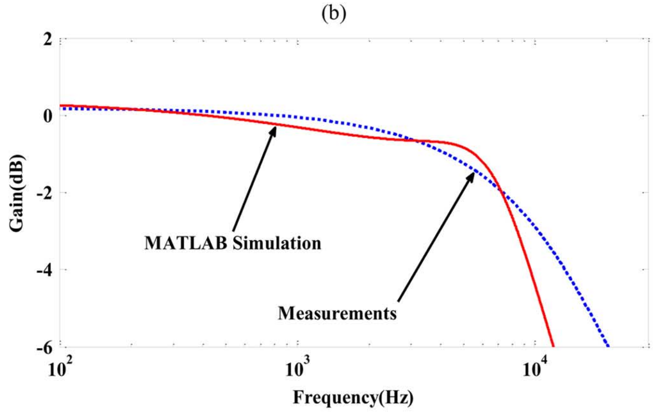

(c)

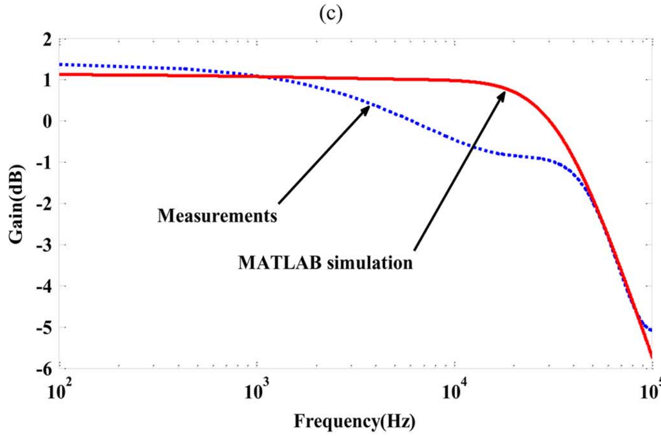

(d)

Fig. 11. (a) Realized fractional order elements, (b) the realized fractional order KHN filter, (c) KHN filter experimental measurements for $\alpha = 0.7, \beta = 1.2$, (d) KHN filter experimental measurements for $\alpha = 0.7$ and $\beta = 0.7$.

condition for Butterworth filter. Then the relation between the transfer function parameters $\{\mathrm{a}, \mathrm{b}, \mathrm{c}\}$ and the circuit elements is obtained from Table I. As shown in Fig. 10(b), the filter response is maximally flat in the pass-band which confirms the discussion

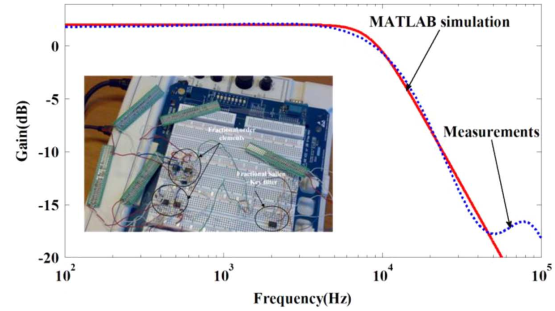

(a)

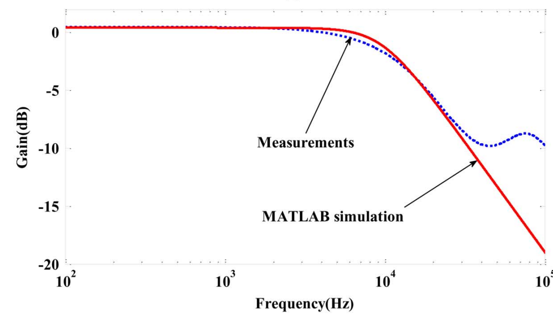

(b)

Fig. 12. (a) Sellen–Key filter experimental measurements for $\alpha = 1.2$ and $\beta = 1.5$. (b) Sellen–Key filter experimental measurements for $\alpha = 1.2$ and $\beta = 0.7$.

mentioned before. Besides, the simulation results are similar to the numerical analysis. While the procedure of [11] cannot design a fractional order filter of transfer function similar to (6) like the Sallen–Key filter, the proposed design can now design such filters.

IV. Experimental Work

Fractional order capacitors of the orders 0.5, 0.7, and 0.8 are realized using the domino ladder network of [26]. These fractional order elements are used to realize fractional elements of the order 1.2 and 1.5 by using the GIC structure. A demonstrative image of the realized fractional order elements are shown in Fig. 11(a). The fractional order capacitors were designed to work in the frequency range 5–60 kHz with a phase error of approximately ± 3 degrees. Hence, this region was chosen for the operation of the filters. The fractional order KHN filter is constructed by replacing the two capacitors with two fractional order capacitors, as shown in Fig. 11(b). The fractional order filter was realized to work at a cutoff frequency of 10 kHz. To realize the filters, TL082 op-amp is used. In addition, the kit of NI ELVIS II^{+} from national instrument is used for measuring the outputs. The kit works at a sample rate of 100 MS/s and configured to take 300 reading per decade. The measured data for the fractional order filter of the orders $(\alpha, \beta) = (0.7, 1.2)$ and $(\alpha, \beta) = (0.7, 0.7)$ is presented in Fig. 11(c) and (d), respectively, after using the basic fitting techniques of the seventh order for the measured data. As illustrated in Fig. 11(c) and (d), there is a deviation between the numerical analysis and the experimental work. It is expected that this deviation is due to the nonlinearity of the op-amps as the fractional order KHN filter uses about seven op-amps. In addition, the floating GIC used in the circuit also adds an extra nonlinearity. So, the fractional order KHN filter satisfies the requirements of Butterworth. Besides, the slopes of the measured data and the numerical analysis are very close.

This means that the practical filters give the expected fractional orders. In addition, the fractional order Sallen–Key filter is also tested and the image of the circuit is shown in the subplot of Fig. 12(a). Alongside the measured data, the MATLAB simulations are also presented for the orders $(\alpha, \beta) = (1.2, 1.5)$ and $(\alpha, \beta) = (1.2, 0.7)$ in Fig. 12(a) and (b). A great matching between the experimental work and the numerical analysis appeared as depicted in Fig. 12(a) and (b). Also, the slopes of the measured data and the numerical analysis are very similar for both cases ($-20(\alpha + \beta)$ dB/s). Thus, the practical fractional order Sallen–Key filters give the expected fractional order response.

V. Conclusion

This paper introduces the necessary and sufficient condition to achieve the Butterworth filter response in the fractional order domain where the conventional case is a special case. This condition has been derived analytically, validated through numerical simulations, and also by experimental results. Different passive and active fractional-order Butterworth filter have been discussed and verified experimentally. Moreover, it becomes possible to control the filter poles and the bandwidth without affecting the circuit components by changing the fractional orders.

References

[1] R. Caponetto, G. Dongola, L. Fortuna, and I. Petráš, *Factional Order System—Modeling and Control Applications*. Singapore: World Scientific Publishing, 2010.

[2] K. B. Oldham and J. Spanier, *The Fractional Calculus*. New York: Academic, 1974.

[3] I. Podlubny, *Fractional Differential Equations*. New York: Academic, 1999.

[4] K. Miller and B. Ross, *An Introduction to the Fractional Calculus and Fractional Differential Equations*. New York: Wiley, 1993.

[5] H. Li, Y. Luo, and Y. Q. Chen, “A fractional-order proportional and derivative (FOPD) motion controller: Tuning rule and experiments,” *IEEE Trans. Control Syst. Tech.*, vol. 18, no. 2, pp. 516–520, 2010.

[6] S. Mukhopadhyay, C. Coopmans, and Y. Q. Chen, “Purely analog fractional-order PI control using discrete fractional capacitors (Fractals): Synthesis and experiments,” in *Proc. Int. Design Eng. Tech. Conf. Comput. Inf. Eng. Conf.*, 2009.

[7] A. G. Radwan, A. M. Soliman, and A. S. Elwakil, “First-order filters generalized to the fractional domain,” *J. Circuits, Syst., Comput.*, vol. 17, no. 1, pp. 55–66, 2008.

[8] A. G. Radwan, A. S. Elwakil, and A. M. Soliman, “On the generalization of second order filters to the fractional order domain,” *J. Circuits, Syst., Comput.*, vol. 18, no. 2, pp. 361–386, 2009.

[9] A. Soltan, A. G. Radwan, and A. M. Soliman, “Fractional order filter with two fractional elements of dependant orders,” *Microelectron. J.*, vol. 43, no. 11, pp. 818–827, 2012.

[10] A. Soltan, A. G. Radwan, and A. M. Soliman, “Butterworth passive filter in the fractional-order,” presented at the 23rd Int. Conf. Microelectron., Tunis, Tunisian , 2011.

[11] T. J. Freeborn, B. Maundy, and A. S. Elwakil, “Field programmable analogue array implementation of fractional step filters,” *IET Circuits Devices Syst.*, vol. 4, no. 6, pp. 514–524, 2010.

[12] A. G. Radwan, A. S. Elwakil, and A. M. Soliman, “Fractional-order sinusoidal oscillator: Design procedure and practical examples,” *IEEE Trans. Circuits Syst.*, vol. 55, no. 7, pp. 2051–2063, Jul. 2008.

[13] D. Mondal and K. Biswas, “Performance study of fractional order integrator using single-component fractional order element,” *IET Circuits Devices Syst.*, vol. 5, no. 4, pp. 334–342, 2011.

[14] A. G. Radwan and K. N. Salama, “Passive and active elements using fractional $L_\beta C_\alpha$ circuit,” *IEEE Trans. Circuits Syst. I*, vol. 58, no. 10, pp. 2388–2397, Oct. 2011.

[15] A. G. Radwan, “Stability analysis of the fractional-order RLC circuit,” *J. Fractional Calculus Appl.*, vol. 3, 2012.

[16] A. G. Radwan, A. M. Soliman, A. S. Elwakil, and A. Sedeek, “On the stability of linear systems with fractional-order elements,” *Chaos, Solitons Fractals*, vol. 40, pp. 2317–2328, 2009.

[17] A. G. Radwan, K. Moddy, and S. Momani, “Stability and nonstandard finite difference method of the generalized Chua’s circuit,” *Comput. Math. Appl.*, vol. 62, pp. 961–970, 2011.

[18] T. C. Doehring, A. H. Freed, E. O. Carew, and I. Vesely, “Fractional order viscoelasticity of the aortic valve: An alternative to QLV,” *J. Biomech. Eng.*, vol. 127, no. 4, pp. 700–708, 2005.

[19] I. S. Jesus, T. J. A. Machado, and B. J. Cunha, “Fractional electrical impedances in botanical elements,” *J. Vibrat. Control*, vol. 14, no. 9, pp. 1389–1402, 2008.

[20] M. Faryad and Q. A. Naqvi, “Fractional rectangular waveguide,” *Progress Electromagn. Res.*, vol. 75, pp. 384–396, 2007.

[21] A. Shamim, A. G. Radwan, and K. N. Salama, “Fractional smith chart theory and application,” *IEEE Microwave Wireless Compon. Lett.*, vol. 21, no. 3, pp. 117–119, Mar. 2011.

[22] A. G. Radwan, A. Shamim, and K. N. Salama, “Theory of fractional-order elements based impedance matching networks,” *IEEE Microwave Wireless Compon. Lett.*, vol. 21, no. 3, pp. 120–122, Mar. 2011.

[23] M. Sugi, Y. Hirano, and K. Saito, “Simulation of fractal immittance by analog circuits: An approach to the optimized circuits,” *IEICE Trans. Fund.*, vol. E82-A, no. 8, pp. 1627–1635, 1999.

[24] R. L. Magin, *Fractional Calculus in Bioengineering*. Redding, CT: Begell House, 2006.

[25] K. Moaddy, A. G. Radwan, K. N. Salama, S. Momani, and I. Hashim, “The fractional-order modeling and synchronization of electrically coupled neurons system,” *Comput. Math. Appl.*, vol. 34, no. 10, pp. 3329–3339, 2012.

[26] B. T. Krishna, “Studies on fractional order differentiators and integrators: A survey,” *Signal Process.*, vol. 91, pp. 386–426, 2011.

[27] M. Nakagawa and K. Sorimachi, “Basic characteristic of fractance device,” *IEICE Trans. Fund.*, vol. E75-A, no. 12, pp. 1814–1819, 1992.

[28] K. Saito and M. Sugi, “Simulation of power low relaxation by analog circuits: Fractal distribution of relaxation times and non-integer exponents,” *IEICE Trans. Fund.*, vol. E76-A, no. 2, pp. 204–209, 1993.

[29] B. T. Krishna and K. V. V. S. Reddy, “Active and passive realization of fractance device of order 1/2,” *Active Passive Electron. Compon.*, vol. 2008, pp. 1–5, 2008.

[30] A. S. Sedra and P. O. Brackett, *Filter Theory and Design: Active and Passive*. , New York: Wiley, 1986, pp. 1–100.

[31] L. Thede, *Practical Analog and Digital Filter Design*. Boston, MA: Artech House, 2004, pp. 15–54.

[32] S. Winder, *Analog and Digital Filter Design*. New York: Newnes, 2002, pp. 41–122.

[33] S. Butterworth, “Theory of filter amplifier,” *Exp. Wireless Wireless Eng.*, vol. 7, pp. 536–541, 1930.

A. Soltan Ali received the B.Sc. and M.Sc. degrees from the University of Cairo, Cairo, Egypt, in 2004 and 2008, respectively, and is currently working towards the Ph.D. degree in electronics and communication at Cairo University, Cairo, Egypt.

He is currently working as a Teacher Assistant in Department of Electronics and Communications Engineering, Fayoum University, Fayoum, Egypt, since his graduation. His current research interests include the investigation of fractional circuits and systems, specifically in fractional order analog filters for signal processing. Also he is interested in the analog circuits with particular emphasis on current-mode approach, RF power amplifiers, and VCO.

Ahmed G. Radwan (SM'12) received the B.S. (with honors), M.S., and Ph.D. degrees in electronics engineering from Cairo University, Cairo, Egypt, in 1997, 2002, and 2006, respectively.

His main research interests are in the fields of nonlinear circuit analysis, chaotic systems, fractional order systems, and memristor-based circuits. He is an Associate Professor in the Engineering Mathematics Department and the Director of the Technical Center for Job Creation (TCJC), Cairo University, Egypt. In addition, he is with the Nanoelectronics Integrated Systems Center (NISC), Nile University, Egypt. From 2008 to 2009, he was invited as a Visiting Professor with the Computational Electromagnetics Lab, ECE, McMaster University, Hamilton, ON, Canada. In 2010, he was recruited to be one of the pioneer researchers at King Abdullah University of Science and Technology (KAUST), Saudi Arabia, conducting research there through 2012. He introduced many generalized theorems applicable to fractional order circuits and electromagnetics. He is the co-author of more than 85 papers and five patents.

Dr. Radwan received the best thesis award from Cairo University in 2002.

Ahmed M. Soliman (LSM'09) was born in Cairo Egypt, on November 22, 1943. He received the B.Sc. degree with honors from Cairo University, Cairo, Egypt, in 1964, the M.S. and Ph.D. degrees from the University of Pittsburgh, Pittsburgh, PA, USA, in 1967 and 1970, respectively, all in electrical engineering.

He is currently Professor Electronics and Communications Engineering Department, Cairo University, Cairo, Egypt. From September 1997 to September 2003, he served as Professor and Chairman Electronics and Communications Engineering Department, Cairo University, Egypt. From 1985 to 1987, he served as Professor and Chairman of the Electrical Engineering Department, United Arab Emirates University, and from 1987 to 1991 he was the Associate Dean of Engineering at the same University. He has held visiting academic appointments at San Francisco State University, Florida Atlantic University, and the American University in Cairo. He was a visiting scholar at Bochum University, Germany (Summer 1985) and with the Technical University of Wien, Austria (Summer 1987). He is Associate Editor of the *Journal of Circuits, Systems and Signal Processing* from January 2004 to present. He is Associate Editor of the *Journal of Advanced Research* Cairo University.

Dr. Soliman was decorated with the First Class Science Medal, from President El-Sadat of Egypt, for his services to the field of Engineering and Engineering Education, in 1977. In 2008, he received the State Engineering Science Excellency Prize Award from the Academy of Scientific Research Egypt. In 2010, he received the State Engineering Science Appreciation Prize Award from the Academy of Scientific Research Egypt. He is a member of the Editorial Board of the IET Proceedings Circuits Devices and Systems. He is a Member of the Editorial Board of Electrical and Computer Engineering (Hindawi). He is a Member of the Editorial Board of Analog Integrated Circuits and Signal Processing. He is also a Member of the Editorial Board of Scientific Research and Essays. He served as Associate Editor of the IEEE TRANSACTIONS ON CIRCUITS AND SYSTEMS—PART I from December 2001 to December 2003. In 2013, he was decorated with the First Class Science Medal, from the President of Egypt, for his services to the country.